

A Novel Dual-band Electromagnetic Bandgap for WLAN Applications

Huynh Nguyen Bao Phuong¹, Dao Ngoc Chien¹, and Tran Minh Tuan²

¹ School of Electronics and Telecommunications, Hanoi University of Science and Technology

² Ministry of Information and Communications of Socialist Republic of Vietnam

E-mail: phuonghnb-set@mail.hut.edu.vn

Abstract: A novel dual-band electromagnetic bandgap (EBG) for wireless local area network (WLAN) applications is designed in this paper. The EBG structure is based on hexagonal geometry and does not use via or multilayer. The bandgap characteristics are investigated by determining the scatter parameters. By adjusting the parameters in the dimension of the structure, the dual bandgaps can be controlled easily to achieve the WLAN frequencies. Comparisons between the proposed structure with another one, which have the same dielectric permittivity and thickness of the dielectric substrate, have been done. The structure is then also optimized to obtain the high impedance in surface at the frequencies of the WLAN bands, which are centered at 2.45 GHz and 5.5 GHz. Simulated and measured results are shown to demonstrate the performance of the proposed structure.

I. INTRODUCTION

Recently, high impedance surfaces (HIS) have attracted considerable attention to improve antenna's performance. High impedance surfaces have two main possible behaviours: artificial magnetic conductor (AMC) properties and electromagnetic bandgap (EBG) properties that lead to the surface wave suppression and in-phase reflection coefficient properties [1-3]. EBG structure is a periodical cell included of a metallic or dielectric element. The unique characteristic of EBG structures is to exhibit bandgap feature in the suppression of surface wave propagation. Many studies have been carried out in EBG structures. Several EBG structures have been proposed for applications in the electromagnetic and antennas community [4-6].

Practical applications of EBG structure usually have difficulty in accommodating its physical size,

because the period of EBG lattices has to be a half-wavelength at the bandgap frequency. This problem has not been solved until the mushroom-like EBG proposed by Sievenpiper et al. [7]. However, the mushroom EBG structure has large size when operating at low frequencies. The requirements of the EBG structures in most microwave applications are a small unit cell size. In addition, the increasing of demand on designing multi-band EBG structures for multi-band applications. Some of dual bandgap EBG structures were found in the literature [8-10]. In [8], two EBG structures with different shape are used. A pair of L-shaped slots and U-shaped is etched on the metal surface of an EBG structure is proposed in [9, 10]. In [11], a triple-band EBG constructed by etching a complementary split ring resonator on the patch of a conventional mushroom-type EBG is proposed. However, these EBG structures were investigated by using via which is more complex in fabrication. Besides, a cascaded EBG of ten unit cells was proposed to introduce dual bandgaps [12]. In which, the vias are moved off the center of six patches and placed at the center of four rest ones. Therefore, this EBG structure also enlarged the total size of the structure. In order to overcome these problems, a planar dual-band EBG structure is proposed in this paper. The structure is constructed on a hexagonal geometry, which is supported for independent polarization.

In Section II, the initial design of dual-band EBG structure is firstly proposed and investigated. The aiming of these bandgaps in this work is covering the range of WLAN bands. The bandgap characteristics of the proposed design are analyzed in Section III. The

structure is optimized to having the high impedances in surface at 2.45 GHz and 5.5 GHz, which are the center frequencies of WLAN bands. Next, the measurement of the proposed EBG structures in fabrication and discussions are also utilized. Finally, the conclusion is given in Section IV.

II. DUAL BAND EBG DESIGN

The resonant frequency and the bandwidth of an EBG structure depend on the unit-cell geometry together with substrate's relative dielectric permittivity and thickness. Each unit cell implements a distributed parallel network having one or more resonant frequencies. The resonant frequency is where the high impedance conditions occur, and for a parallel circuit is defined as follows [6]:

$$f_c = \frac{1}{2\pi\sqrt{LC}} \quad (1)$$

In theory, in order to construct a dual-band EBG structure, it is necessary to create two LC equivalent circuits separately. The center frequency of the bandgap will be determined based on the values of L and C of these equivalent circuits. Besides, the center frequency can be customized to achieve the desired value. The proposed structure is presented in Fig.1, which is printed on a FR4 dielectric slab with dielectric constant of 4.4 and a thickness of 1.6 mm and loss tangent of 0.02. Dark parts in this figure represent the metallic periodic structure, which is etched on a grounded dielectric substrate. Unit cell dimension is $W = 8.25$ mm and the metallization thickness is $18 \mu\text{m}$. The EBG structure designing include two steps. Step one is created the first bandgap. In this step, six straight lines and six arrow-shaped line was formed. The second step has been done to obtain the second bandgap. Three V-shaped lines are added to the initial arrow-shaped line. As the results, the EBG structure included six straight lines and six arrow-shaped lines, which contain four V-shaped lines. Generally, this EBG structure looks like a net-shaped.

From this design, the proposed EBG structure can be represented by two different equivalent circuits, which are shown in Fig. 2. The first bandgap is

formed, as the principle of uni-planar compact EBG (UC-EBG) that was proposed by F. Yang in [13], by using the straight lines and the gaps between two outmost V-shaped strips of two adjacent cells (see Fig. 2a). These straight lines, which are connecting two consecutive cells, introduce the equivalent inductance L_1 ; while the gaps (2G) introduce the equivalent capacitance C_1 . The center frequency of the first bandgap can be estimated as follows:

$$f_{c1} = \frac{1}{2\pi\sqrt{L_1(2C_1)}} \quad (2)$$

Equivalent circuit of the second bandgap is defined by the L and C element those are formed inside the EBG structure. Firstly, the equivalent inductance L_2 is formed by the arrow-shaped strip lines. Then the equivalent capacitance C_2 is generated by the gap between the V-shaped strips. Thus, the capacitance C_2 is total of the series of the equivalent capacitances C_{pi} , which is the parasitic capacitance. Finally, the central frequency of the second bandgap of equivalent circuit shown in Fig. 2(b) can be expressed:

$$f_{c2} = \frac{1}{2\pi\sqrt{L_2C_2}} = \frac{1}{2\pi\sqrt{L_2 \cdot 2\left(\sum_{i=1}^3 \frac{1}{C_{pi}}\right)^{-1}}} \quad (3)$$

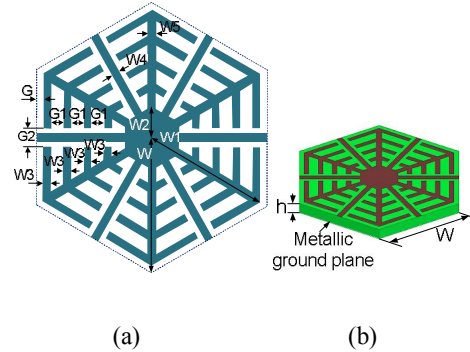


Figure 1. EBG structure: a. Proposed EBG structure; b. Slide view of the EBG structure

After the investigating of the equivalent circuits of the structure has been done, the initial design of the EBG structure is made. The main purpose of this section is two-bandgap procedure, which is covering the frequency ranges of the WLAN. The initial parameters of the structure are detailed in Table 1. In

order to analyze the bandgap properties of the EBG structure with a finite unit number, an experiment concerning transmission through the above EBG structure has been carried out [13]. CST numerical simulation was used to simulate the EBG structure. A 3×4 lattice of the unit cell is mounted on a grounded dielectric slab and connected with 50Ω micro-strip lines at both ends as the filter structure (See Fig.3). When the surface waves propagation throughout these structures, the energy of the waves will be reflected almost completely. Therefore, the structures act as well as a stop-band filter. The bandgap bandwidth will be defined with S_{11} is above -5 dB and S_{21} is below -30 dB at the same time.

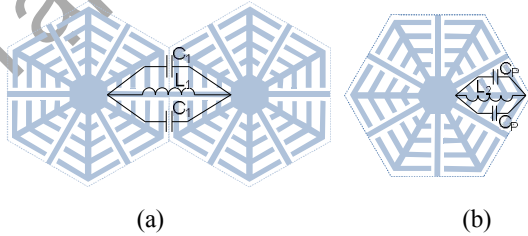


Figure 2. Equivalent circuits of the proposed structure: a. First bandgap; b. Second bandgap

Table 1. Initial parameters of structure (mm)

W	W ₁	W ₂	W ₃	W ₄
8.25	7.95	2	0.5	0.5
W ₅	G	G ₁	G ₂	h
0.5	0.25	0.5	1.2	1.6

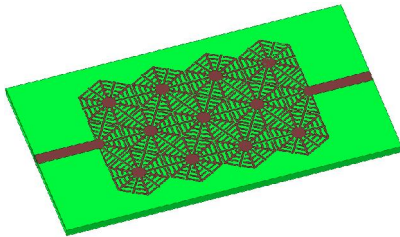


Figure 3. The geometry of 3×4 EBG array connected with two micro-strip lines at both ends

Simulated result of bandgaps of the initial structure design is presented in Fig. 4. As can be seen from Fig. 4, the first bandgap is centered at 2.76 GHz and spans the frequencies from 2.25 to 3.27 GHz, while the higher one spans the frequencies from 4.32 to 6.08

GHz with center frequency located at 5.2 GHz. From the standard for WLAN applications, IEEE 802.11b/g/a, covers frequency bands of 2.40-2.48 GHz and 5.2-5.8 GHz. It is clear that both bandgaps of the EBG structure have met the WLAN requirements. However, the center frequencies of the bandgaps are not overlapping the center frequencies of the WLAN. This means that the surface impedance has not reached maximum at the center frequencies of WLAN. Therefore, the bandgap characteristics of the proposed EBG structure are not useful in this situation.

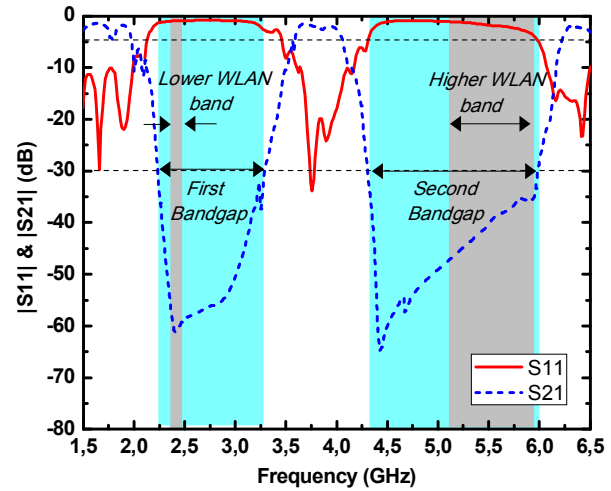


Figure 4. Dual bandgaps of initial structure design

III. BANDGAP CHARACTERISTICS

In this section, the EBG structure will be optimized according to the parameters to achieve high impedances in surface at the center frequencies of the WLAN bands. Thus, as seen in Fig. 4, it is necessary to reduce f_{c1} and increase f_{c2} . Generally, it can be adjusted the center frequency by changing the values of equivalent capacitance C or equivalent inductance L . In the EBG design procedure, if the dielectric material and its thickness have been chosen, the total equivalent inductance L cannot be altered. Therefore, only capacitance C can be changed.

From the equation (2), the frequency f_{c1} is reduced when the value of capacitance C_1 is increased. This can be done by reducing G , which is the gap between

two outmost V-shaped strips of two adjacent cells. Indeed, as can be seen from Fig. 5, the first bandgap move to lower region as G move to lower value. This is a perfect fit in theoretically, because the gap G and the capacitance C_1 are always inversely proportional to each other. Besides, f_{C2} almost unchanged when we are adjusting the value of f_{C1} .

Similarly, the center frequency of the second bandgap can be adjusted by the capacitance C_{P1} in the equation (3). There are two parameters affecting directly to the value of C_{P1} . First, it is the gap G_1 between the parallel V-shaped strip lines; second, that is the gap G_2 between the terminals of the strip lines, which are placed symmetrically through the straight line. Fig. 6 presents the simulated bandgaps of the EBG structure with variations of G_1 . It is seen that the second bandgap moves to the higher region by increasing the value of G_1 . This is entirely consistent with the equation (3), when G_1 increases the C_{P1} will be reduced leading to the increasing of f_{C2} . Next, the effect of G_2 to the center frequency of the second bandgap is investigated. As observed in Fig. 7, the second bandgap also moves to higher region when the value of G_2 is increasing. Actually, the increasing of G_2 leads to the length decreasing of the V-shaped strip lines. This means that the value of C_{P1} is also decreased. Besides, when we change the value of G_1 and G_2 in order to shift this bandgap the first bandgap almost unchanged. This proves that f_{C1} and f_{C2} is completely independent of each other and can be adjusted easily.

Tables 2 render important information to compare the proposed EBG design with other ones in terms of center frequency and bandgap bandwidth. To analyze the influence of the EBG unit-cell geometry itself, a comparison between unit cells with the same relative dielectric permittivity and thickness is carried out. From Table 2, it is observed that for $\epsilon_r = 2.2$ of $h = 2$ mm comparing unit cells of 7.5 mm, the simulated EBG operation bandwidths for a complementary slip resonator EBG [11] are 27.4 % and 6.3 %, whereas for the presented hexagonal design are 36.6 % and 31.5 %. In case of unit cell of 10 mm, for $\epsilon_r = 4.7$ of $h = 1.6$ mm the bandwidth for a pair L-shaped slots [9] are 21.5 % and 25.4 %, while for proposed EBG are

46.9% and 39.1%. Comparing unit cell having the size of 11 mm [10] (24.8% and 14.8 %) with the novel design (42.4% and 49.2 %) for $\epsilon_r = 4.9$ of $h = 1.6$ mm, it can be seen that the proposed EBG design exhibits wider EBG operation bandwidth in all cases. Besides, the center frequencies of the proposed design are almost smaller than that of other ones. It can be concluded that the novel EBG structure is more compact in size in all cases.

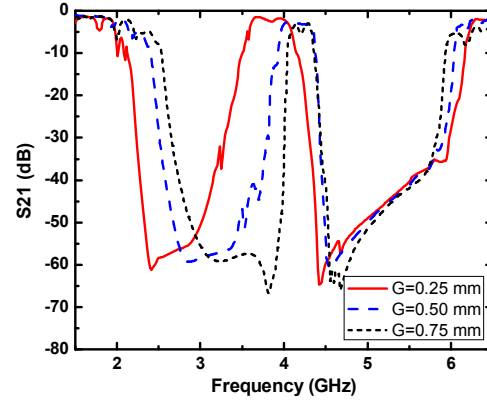


Figure 5. Simulated results of S_{21} for different values of G when $G_1=0.5$ mm and $W=8.25$ mm.

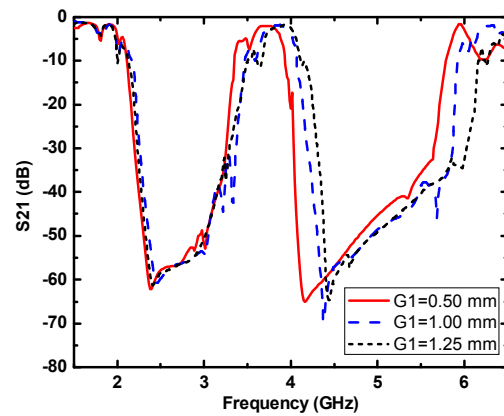


Figure 6. Simulated results of S_{21} for different values of G_1 when $G_2=1.2$ mm and $W=8.25$ mm.

Finally, the bandgaps has been optimized according to the goal of this section. The optimized parameters are summarized in Table 2. The simulated results of the bandgap are shown in Fig. 10. As can be observed from Fig. 10, the first bandgap spans the frequencies from 2.08 to 2.94 GHz while the second

Table 2. Unit cells comparison between the proposed EBG with other EBG structures.

Reference	Unit cell size (mm)	Thickness (mm)	ϵ_r	Bandgap 1		Bandgap 2	
				Reso.Freq (GHz)	BW (%)	Reso.Freq (GHz)	BW (%)
[9]	10	1.6	4.7	2.37	21.5	6.66	25.4
[10]	11	1.6	4.9	2.33	24.8	5.12	14.8
[11]	7.5	2.0	2.2	3.83	27.4	5.67	6.3
This paper	10	1.6	4.7	1.79	46.9	4.04	39.1
	11	1.6	4.9	1.65	42.4	3.41	49.2
	7.5	2.0	2.2	3.04	36.6	6.22	31.5

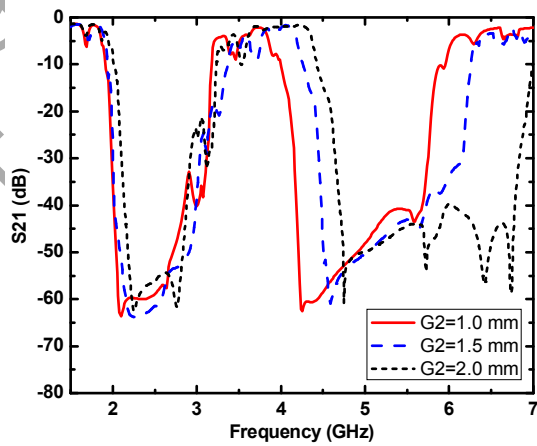


Figure 7. Simulated results of S_{21} for different values of G_2 when $G_1=1$ mm and $W=8.25$ mm.

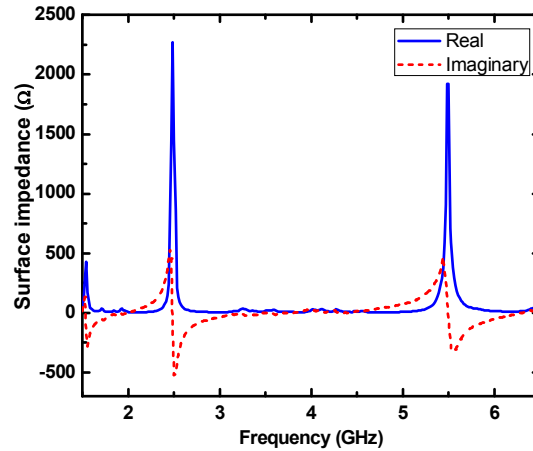


Figure 8. Simulated results of surface impedance of the optimized EBG structure

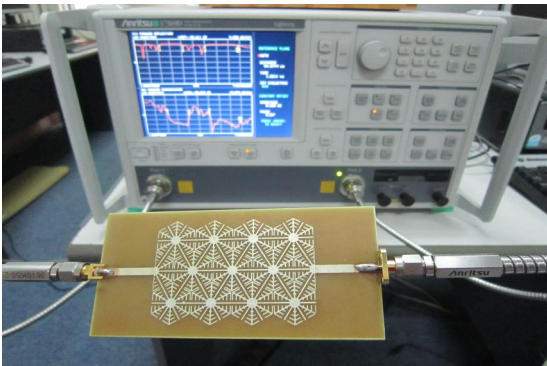


Figure 10. Photograph and measurement set up of an array of 3×4 proposed EBG unit cell

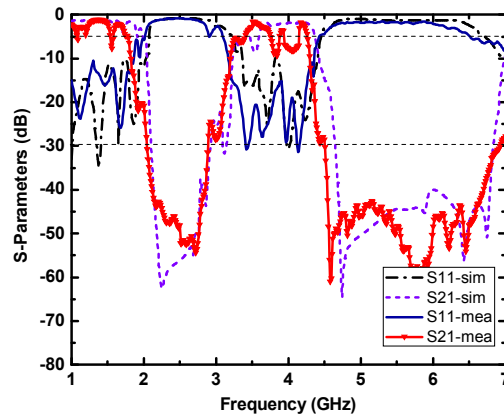


Figure 11. Results of S -parameters of the optimized EBG structure

bandgap spans the frequencies from 4.64 to 6.68 GHz. The optimized surface impedance of the EBG structure is shown in Figure 8. As can be seen from

Fig. 8, the structure has high surface impedance at 2.45 GHz and 5.5 GHz.

In order to validate the design of the proposed EBG structure, a prototype of an array of 3×4 EBG unit cell has fabricated and measured. The micro-strip lines of the fabricated structure are soldered with SMA connector to measure the scatter parameters. The experimental measurements of the structure are performed by Anritsu 37369D network analyzer. A photo of the fabricated array is presented in Fig. 9, while the measured results of scatter parameters are also presented in Fig. 10. It is seen that the simulated and measured results are in accordance with together.

Table 3. Optimized parameters of structure (mm)

W	W₁	W₂	W₃	W₄
8.25	8.07	2	0.5	0.5
W₅	G	G₁	G₂	h
0.5	0.15	1	2	1.6

IV. CONCLUSION

A novel dual-band planar EBG structure for WLAN application has been designed in this paper. The structure can be represented by two different equivalent circuits LC. The bandgaps can be controlled easily by changing the parameters in dimension. Comparisons between the proposed structure with the other ones are demonstrated the wider bandwidth and the compactness of the proposed design. The structure has been optimized for having the high impedance surface at 2.45 GHz and 5.5 GHz, which are the center frequencies of the WLAN bands. Simulated and measured results are shown to demonstrate the performance of the EBG structure. Because the structure is small size, easy fabrication and low cost, it can be used for WLAN systems as a high impedance ground plane for reducing back radiation and increasing radiation efficiency.

REFERENCES

- [1] O. Folyan and R. Langley, "Dual frequency band antenna combined with a high impedance band gap surface," *IET Microwaves, Antennas Propag.*, vol. 3, no. 7, pp. 1118–1126, 2009.
- [2] G. Goussetis, A. P. Feresidis, and J. C. Vardaxoglou, "Tailoring the AMC and EBG characteristics of periodic metallic arrays printed on grounded dielectric substrate," *IEEE Trans. Antennas Propag.*, vol. 54, no. 1, pp. 82–89, Jan. 2006.
- [3] F. Yang and Y. Rahmat-Samii, "Microstrip antennas integrated with electromagnetic bandgap (EBG) structures: A low mutual coupling design for array applications," *IEEE Trans. Antenna Propag.*, vol. 51, no. 10, pp. 2936–2946, Oct. 2003.
- [4] F. Yang and Y. Rahmat-Samii, "Electromagnetic Bandgap Structures in Antenna Engineering", Cambridge, U.K: Cambridge Univ. Press, 2008.
- [5] C. Cheype, C. Serier, M. Thevenot, T. Monediere, A. Reineix, and B. Jecko, "An electromagnetic bandgap resonator antenna," *IEEE Trans. Antennas Propag.*, vol. 50, no. 9, pp. 1285–1290, Sep. 2002.
- [6] L. Yang, M. Fan, F. Chen, J. She, and Z. Feng, "A Novel Compact Electromagnetic-Bandgap (EBG) Structure and Its Applications for Microwave Circuits," *IEEE Trans. Microw. Theory Tech.*, vol.53, no. 1, pp. 183-190, Jan. 2005.
- [7] D. Sievenpiper, L.J. Zhang, R. F. J. Broas, N. G. Alexopolous, and E. Yablonovitch, "High-impedance electromagnetic surface with a forbidden frequency band," *IEEE Trans. Microw. Theory Tech.*, vol. 47, no. 11, pp. 2059-2074, Nov. 1999.
- [8] W. Wang, X. Cao, R. Wang, J. Ma, "A Small Dual-band EBG Structure for Microwave," *International Conference on Microwave and Millimeter Wave Technology*, Nanjing, China. 2008.
- [9] O. Ayop, M. A. Rahim, and T. Masri, "A Dual Band Gap Slotted Patch Electromagnetic Band Gap for Dual Band Microstrip Antenna," *International RF and Microwave Conference*, Kuala Lumpur, Malaysia. 2008.
- [10] O. Ayop, M. A. Rahim, and T. Masri, "Dual Band Electromagnetic Band Gap (EBG) Structure," *Asia-Pacific Conference on Applied Electromagnetic*, Melaka, Malaysia. 2007.
- [11] L. Peng, C. L. Ruan and Z. Q. Li, "A Novel Compact and Polarization-Dependent Mushroom-Type EBG Using CSRR for Dual/Triple-Band applications," *IEEE Microw. Wireless Compon. Lett.*, vol. 20, no. 9, pp. 489–491, Sep. 2010.
- [12] L. J. Zhang, C.-H. Liang, L. Liang, and L. Chen, "A Novel Design Approach For Dual-Band Electromagnetic Bandgap Structure" *Progress In Electromagnetics Research M*, vol. 4, 81–91, 2008.
- [13] F. R. Yang, K. P. Ma, Y. X. Qian, and T. Itoh, "A uniplanar compact photonic-bandgap (UC-PBG) structure and its applications for microwave circuit," *IEEE Trans. Microw. Theory Tech*, vol. 47, no. 8, pp.1509–1514, Aug. 1999.
- [14] B.Q. Lin, Q.R. Zheng and N.C. Yuan, "A novel planar PBG structure for size reduction," *IEEE Microw. Wireless Compon. Lett.*, vol. 16, no. 5, pp. 269–271, May. 2006.

AUTHOR'S BIOGRAPHIES



Huynh Nguyen Bao Phuong received the B.E and M.Sc. degrees in 2003 and 2007, respectively, from School of Electronics and Telecommunications, Hanoi University of Science and Technology, Vietnam. Now he is a Lecturer of the Faculty of Technique and Technology, Quynhon University, Vietnam. Currently, he is working toward Ph.D degree at the School of Electronics and Communications, Hanoi University of Science and Technology, Vietnam.

His research interests are high impedance surfaces (HIS), ultra wideband (UWB), microstrip and metamaterial antennas.



Tran Minh Tuan (Assoc. Prof. Ph.D) was born in Hanoi – Vietnam in 1970. He received the B.E degree and M.E degree in Satellite Communications from Moscow Institute of Technology in Russia in 1994 and in 1995, respectively. In 2004, he received Ph.D degree in antenna and radiowave propagation in Hanoi University of Science and Technology, Vietnam. Now he is Vice President of National Institute of Information and Communications Strategy, Ministry of Information and Communications of Vietnam.

His current research interests includes: master plans and strategies of telecommunications and IT development in Vietnam, radiowave broadcasting and propagation, slow-wave structures, slotted, leaky-wave and microstrip antennas, CAD software for radio-wave structures, slotted, leaky-wave and microstrip antennas etc.



Dao Ngoc Chien received the Diploma of Engineer in 1997 from the Department of Telecommunication Systems, School of Electronics and Telecommunications, Hanoi University of Science and Technology, where in the same year he became a Teaching Assistant. He received M.Sc. and Ph.D. degrees in 2002 and 2005, respectively, from the Department of Electronics and Computer Engineering, Gifu University, Japan. At the Department of Telecommunication Systems, School of Electronics and Telecommunications, Hanoi University of Science and Technology, he worked as the Senior Lecturer from 2005 to 2011, and is currently the Contracted Lecturer. He has been appointed to Associate Professor since November, 2010.

His research interests include computational electromagnetics based on MoM and FDTD methods, analysis and design of modern antennas and of nanometric

integrated optical circuits based on the surface plasmon polaritons. He has been a reviewer for several journals/transactions of Optical Society of America (OSA), Institute of Electrical and Electronics Engineers (IEEE), Elsevier, and American Geophysical Union (AGU), as well as for a number of conferences. He has been a member of IEEE, OSA and REV.